Preprints of the 21st IFAC World Congress (Virtual)
Berlin, Germany, July 12-17, 2020

An Adaptive Robust Guidance Strategy for Interceptor with Input Quantization

Arunava Banerjee * **Syed Muhammad Amrr** * **M. Nabi** *

* *Department of Electrical Engineering, Indian Institute of Technology Delhi, New Delhi 110016, India. (e-mail: arunavabanerjee27@gmail.com, syedamrr@gmail.com, mnabi@ee.iitd.ac.in).*

Abstract: The computational capabilities of processors have increased many folds over the last few decades. However, due to constraint on space, weight, and cost, the state-of-art onboard processors cannot be generally installed in a missile, which is required to perform multiple parallel computations for a successful interception. An efficient way of minimizing the computational burden can be ensured by reducing the number of updates of the control input, thereby minimizing the load on the onboard processors. A logarithmic quantizer technique is explored in this work for designing a guidance strategy for a two-dimensional interceptor problem. The proposed guidance strategy is capable of tackling disturbances and quantization errors while achieving the primary objective of capturing the target. An adaptive law has also been incorporated to eliminate the need of apriori knowledge about the disturbance bound. Lyapunov theory has been used to show Uniformly Ultimately Bounded (UUB) convergence of the closed-loop system states under the application of the quantized control approach. The proposed scheme is implemented through numerical simulations for the tail-chase and headon engagement scenarios. A comparative analysis of the proposed guidance strategy with the periodic sampling time technique is also included in this work.

Keywords: Quantization, Input Saturation, Adaptive-Robust Control, Uniformly Ultimately Bounded Stability

1. INTRODUCTION

Design of guidance strategies for missiles with high initial heading errors to capture a target have been the subject of interest for a long time (Bezick et al., 1995; Ramesh and Padhi, 2019). A wide range of non-linear control methods like sliding mode control (Shtessel et al., 2007), robust $H2/H\infty$ techniques (Yaghi and Efe, 2019), variable structure control (Moon et al., 2001), PID navigation (Pan et al., 2019), etc., have been applied to efficiently capture the target. Looking beyond the indispensable requirement of interception, the design of modern guidance laws takes into account the effect of disturbance (Gurfil, 2003), reduced updates of control, and also tries to avoid the overuse of control effort (Guo et al., 2019). This work aims at developing a guidance law which addresses all these issues.

At any point during the time of flight, the missile might encounter external disturbances (Gurfil, 2003) which deviates it from the desired path of target interception. This can ultimately lead to either use of more fuel, time or a combination of both. The disturbance might even cause the missile to deviate so far off-course that it might not be able to capture the target. Thus a guidance strategy which will nullify the effects of these disturbances needs to be designed. It can be seen in literature that the upper bound on disturbance is assumed to be known (He et al., 2015) in many works.

In this paper, a Lyapunov based analysis is carried out to design an adaptive-robust guidance scheme which relaxes the assumption of apriori knowledge about the upper bound of disturbance. Subsequently, to reduce the need of continuous data transmission over the communication channel, quantization of the adaptive-robust control input (Li and Yang, 2016) is performed. This leads to significant reduction in computational burden on the onboard processor of the missile and also eliminates the need for continuous update of control law. By reducing the communication load and the updating requirement, the proposed guidance strategy will be an efficient choice for any resource constraint interceptor system. The quantization technique will also help in reducing the weight of onboard heavy wired network. The control law is updated based on the instances when the system requires attention (Xing et al., 2016) rather than as in traditional sampled-data control where continuous sensing and actuation is required periodically.

The quantization parameters are selected in a manner that compliments the controller parameters (Wu and Cao, 2017). The adaptive-robust component of the guidance strategy suppresses the effects of the external disturbances and quantization errors. A detailed Lyapunov analysis of the closed-loop system provided in this work shows UUB stability by selecting appropriate design parameters. Simulation studies are performed on two different scenarios which are the tail-chase and the head-on engagements with

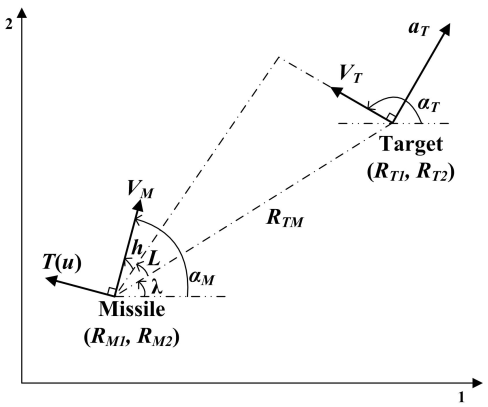

Fig. 1. Two dimensional missile-target engagement

high initial heading errors for the missile. The proposed guidance strategy is shown to work efficiently along with achieving the objectives of interception, disturbance tackling and reduced updating of the control law.

The main contributions of this paper can be summarized as:

- The proposed input quantization based guidance strategy is implemented which makes it suitable for any resource constraint interceptor system.
- The adaptive-robust law is also incorporated in the guidance strategy to tackle the problem of disturbances, noises, and quantization error without apriori knowledge of their upper-bound while achieving the primary objective of intercepting the target.
- The stability analysis of the closed-loop system ensures uniformly ultimately bounded (UUB) stability under the application of the proposed scheme.

2. PROBLEM FORMULATION

In this section, first a brief description of the two-dimensional missile-target engagement model is given, followed by the problem statement.

2.1 Mathematical Model of Missile-Target Engagement

A missile-target engagement scenario having point masses are considered for this work. Both the missile and target maneuver themselves by applying their lateral acceleration which is commonly referred to as *latax*. The target tries to evade the missile while the primary objective of the missile is to capture and destroy the target. A schematic of the 2D interceptor engagement scenario is presented in Fig. 1. The kinematic model can be described as in (Banerjee et al., 2020)

$$\begin{aligned} \dot{\alpha}_T &= a_T/V_T & \dot{\alpha}_M &= \{T(u)/V_M\} + d \\ \dot{R}_{T_1} &= V_T\cos(\alpha_T) & \dot{R}_{M_1} &= V_M\cos(\alpha_M) \\ \dot{R}_{T_2} &= V_T\sin(\alpha_T) & \dot{R}_{M_2} &= V_M\sin(\alpha_M) \end{aligned} \quad (1)$$

The instantaneous direction of motion for the aerial vehicles is represented by their velocity vectors as V_M and V_T. The angles made by these respective velocity vectors with the axis 1 are known as the angle of attack represented as α_M and α_T. The instantaneous position of the target and missile are represented as, $R_T = (R_{T1}, R_{T2})$ and $R_M = (R_{M1}, R_{M2})$ respectively. The heading angle of the missile is represented as the deviation of the flight path angle from its desired value. The heading angle $h \in \mathbb{R}$ is expressed as (Banerjee et al., 2020)

$$h = \alpha_M - (L + \lambda), \quad (2)$$

where the lead angle L is expressed as

$$L = \sin^{-1}[V_T\sin(\alpha_T - \lambda)/V_M], \quad (3)$$

and the Line of sight (LOS) angle λ is given as

$$\lambda = \tan^{-1}[R_{TM2}/R_{TM1}]. \quad (4)$$

The control input command for the missile is the latax $u \in \mathbb{R}$, and the quantized value of latax is denoted by $T(u) \in \mathbb{R}$. The latax is considered to be bounded as in all practical scenarios and the bounds on control are given as $u \in [-\bar{u} \;\; \bar{u}]$. The external disturbances and noise encountered by the missile system are denoted by $d \in \mathbb{R}$.

2.2 Problem Statement

Once the heading angle goes to zero it, in turn, implies that the missile is on-course along a straight-line trajectory to hit the target (Banerjee et al., 2020; Ramesh and Padhi, 2019) without requiring any further corrective maneuver. Also, when the miss distance is in the neighbourhood of zero it signifies that the missile is close enough to the target and the detonation of the missile is carried out. The miss distance is expressed as

$$R_{TM} = \sqrt{{R_{TM_1}}^2 + {R_{TM_2}}^2},$$

Thus, the objective of the guidance strategy is to ensure that:

$$h \to 0, \quad (5)$$

and also to assure that $R_{TM} \approx 0$. In addition to ensuring the primary target of intercepting the target, the proposed guidance strategy has used the quantized input to solve the problem of communication constraint on the wireless transmission channel.

3. LOGARITHMIC QUANTIZER

In the last few years, quantization techniques have been explored to save communication resources in a bandwidth constraint environment while providing significant precision (Wu, 2015). The quantized guidance law proposed in this paper is based on the logarithmic quantizer, which is designed to address this issue of bandwidth constraint on its communication system and is defined as:

$$T(u(t)) = \begin{cases} u_j & \text{if } \frac{u_j}{1+\delta} < u \le \frac{u_j}{1-\delta} \\ 0 & \text{if } 0 \le u \le \frac{u_0}{1+\delta} \\ -T(-u(t)) & \text{if } u < 0, \end{cases} \quad (6)$$

where $u_j = \gamma^{(1-j)}u_0$ for $j = 1, 2, 3, ..., u_0 > 0$, $0 < \gamma < 1$, $\delta = \frac{1-\gamma}{1+\gamma}$, $T(u(t))$ is in the set $U = \{0, \pm u_j\}$, and $u_{\min} = \frac{u_0}{1+\delta}$ determines the size of the dead-zone. The map of $T(u(t))$ for $u > 0$ is shown in Fig. 2. The following remark discusses about the behaviour of the logarithmic quantizer with respect to parameter γ.

Remark 1. The quantization density is measured by the parameter γ and it follows the relation: $\frac{1}{\gamma} = \frac{u_{j+1}}{u_j}$, here $0 < \gamma < 1$. For a larger ratio of $\frac{1}{\gamma} = \frac{u_{j+1}}{u_j}$ a small value of γ is required and thus the sector bound width

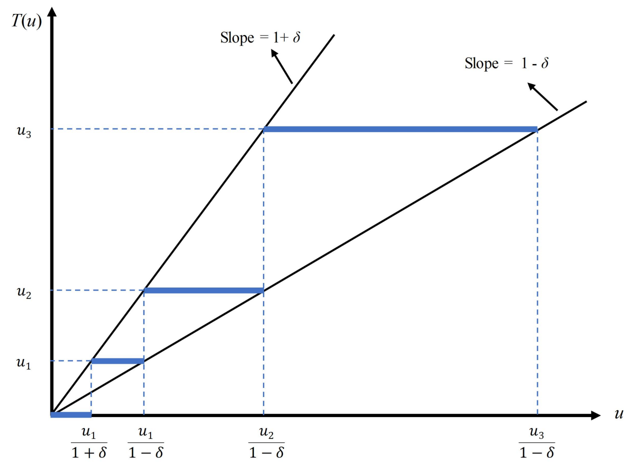

Fig. 2. Quantization map for $u > 0$.

will be large as can be seen from Fig. 2. This, in turn, implies that for a smaller value of γ the quantization will coarser. For a u of fixed length, the $T(u(t))$ will have fewer quantization levels as u varies over this length. This results in lesser communication rates of the control input from the controller module to the actuator module, through the communication channel (Wu, 2015).

Remark 2. The missile system is uncertain about the maneuvering of the target and it also faces external disturbances, thus the parameter γ is not designed in advance. This parameter is chosen in such a manner that it ensures the convergence of the heading error to the neighbourhood of zero.

The logarithmic quantizer $T(u)$ can be expressed into a linear part u and a nonlinear part $z \in \mathbb{R}$ as (Wu, 2015):

$$T(u(t)) = u(t) + z(t), \tag{7}$$

where $z(t) = T(u(t)) - u(t)$. The quantization error $z(t)$ satisfies the following lemma.

Lemma 1. The quantization error $z(t)$ satisfies the following equality (Wu, 2015)

$$\|z(t)\| = \delta\|u(t)\| + u_{\min}. \tag{8}$$

The proof of the above Lemma can be seen from (Wu, 2015).

Assumption 1. The disturbance is assumed to be bounded, i.e., $0 < \|d\| \le \bar{d}$, but the value of $\bar{d}$ is not known apriori.

4. ROBUST ADAPTIVE QUANTIZATION BASED GUIDANCE CONTROL

The basic block diagram of the missile guidance engagement system using quantization technique is shown in Fig. 3. The guidance control command $u(t)$ is fed to the quantizer $T(u(t))$. The quantized value of guidance control input is then fed to the missile actuator via a wireless communication channel. The guidance signal is transmitted as a coded signal using a coder from sending end to the receiving end. The signal gets decoded through a decoder before feeding it to the actuator. It is assumed that the communication channel is free from noises. Some of the expressions which will be used in the convergence proof of heading error are presented below.

Determining the time derivative of h defined in (2) and substituting the value of $\dot{\alpha}_M$ from the missile dynamics (1) yields

$$\dot{h} = \frac{u}{V_M} - \dot{L} - \dot{\lambda} + d + \breve{z}, \tag{9}$$

where $\breve{z} = \frac{z}{V_M}$. The time derivative of L defined in (3), can be expressed as

$$\dot{L} = \frac{V_{TM}\cos(\alpha_T - \lambda)(\dot{\alpha}_T - \dot{\lambda})}{\sqrt{1 - V_{TM}\sin(\alpha_T - \lambda)}}, \tag{10}$$

where $V_{TM} = V_T/V_M < 1$, and the time derivative of λ defined in (4), is given as

$$\dot{\lambda} = \frac{d\lambda}{dt} = \frac{R_{TM_1}V_{TM_2} - R_{TM_2}V_{TM_1}}{{R_{TM}}^2}, \tag{11}$$

It is to be noted that the right-hand side of $\dot{\lambda}$ consists of the distances and constant velocities. Further, it is assumed that the target does not go beyond the reachable domain of the missile at any instant of time. This, in turn, implies that $\dot{\lambda}$ is bounded.

The upper bound value of $\dot{L}$ from (10) can be determined as

$$\begin{aligned}\|\dot{L}\| &\le \left\| \frac{V_{TM}\cos(\alpha_T-\lambda)\{(a_T/V_T)-\dot{\lambda}\}}{\sqrt{1-V_{TM}\sin(\alpha_T-\lambda)}} \right\|, \\ &\le \left\| \frac{V_{TM}\ a_T}{V_T\sqrt{1-V_{TM}}} \right\| + \left\| \frac{V_{TM}}{\sqrt{1-V_{TM}}} \right\| \|\dot{\lambda}\| = a_1 + a_2\|\dot{\lambda}\|, \end{aligned} \tag{12}$$

where $a_1 = \left\| \frac{V_{TM}\ a_T}{V_T\sqrt{1-V_{TM}}} \right\|$ is bounded, $a_2 = \left\| \frac{V_{TM}}{\sqrt{1-V_{TM}}} \right\| < 1$. Moreover, it is already established that $\|\dot{\lambda}\|$ is bounded, therefore $\|\dot{L}\|$ is also bounded.

Now, defining a variable $\mathcal{L}(\cdot) \in \mathbb{R}$ as

$$\mathcal{L}(\cdot) = -\dot{L} - \dot{\lambda} + d + u_{\min}\mathrm{sign}(h). \tag{13}$$

Using Assumption 1, the following inequality can be written as:

$$\|\mathcal{L}(\cdot)\| \le \|\dot{L}\| + \|\dot{\lambda}\| + \bar{d} + u_{\min}. \tag{14}$$

Substituting $\|\dot{L}\|$ from (12) into (14) yields

$$\begin{aligned}\|\mathcal{L}(\cdot)\| &\le a_1 + a_2\|\dot{\lambda}\| + \|\dot{\lambda}\| + \bar{d} + u_{\min}, \\ &\le (a_1 + \bar{d} + u_{\min}) + (a_2 + 1)\|\dot{\lambda}\| = b_1 + b_2\|\dot{\lambda}\| \le b\Theta, \end{aligned} \tag{15}$$

where $b_1 = a_1 + \bar{d} + u_{\min}$, $b_2 = a_2 + 1$, $b = \max\{b_1, b_2\}$, and $\Theta = (1 + \|\dot{\lambda}\|)$.

The proposed adaptive guidance control law is defined as:

$$u = V_M\left\{-kh - \left(\hat{b}(t)\Theta + \mu(t)\right)\frac{h}{\|h\| + \phi}\right\}, \tag{16}$$

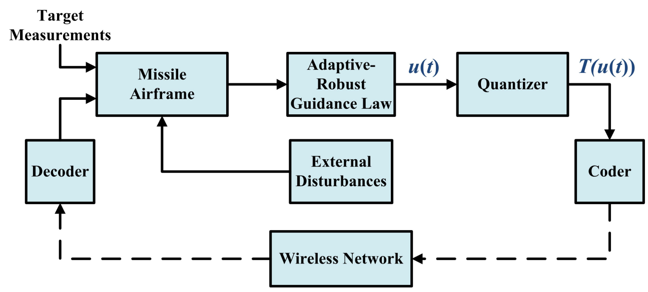

Fig. 3. Schematic block diagram of quantized guidance system

where $\hat{b}(t)$ is the adaptive gain, which is governed as

$$\dot{\hat{b}} = \mathbf{Pr}\left\{\frac{\varsigma\|h\|^2\Theta}{\|h\|+\phi}\right\};\ \mu(t) = \frac{\delta\,\hat{b}(t)\,\Theta}{1-\delta} + \varpi;\ \phi = \frac{\zeta}{1+\Theta},$$

where $\mathbf{Pr}$ represents projection and $k > 0$, $\varsigma > 0$, $\zeta > 0$, and $\varpi > 0$ are design parameters. Moreover, parameter $\hat{b}$ estimates the coefficient b which includes upper bound of d and effect of quantization error.

The following theorem shows the convergence of heading error h.

Theorem 1. Considering that Assumption 1 holds, the heading error in (9) demonstrates uniformly ultimately bounded (UUB) convergence under logarithmic quantization (6) of the proposed controller (16).

Proof. Consider a Lyapunov function $V = 1/2h^2 + (1/2\varsigma)\tilde{b}^2$, where $\tilde{b} = b - \hat{b}$. Substituting the value of $\dot{h}$ from (9) in the time derivative of V to obtain

$$\dot{V} = h\left\{\frac{u(t)}{V_M} - \dot{L} - \dot{\lambda} + d + \check{z}\right\} - \frac{1}{\varsigma}\tilde{b}\dot{\hat{b}}. \tag{17}$$

In view of (8) and $V_M > 1$, $\|h\check{z}\|$ can be written as

$$\begin{aligned}\|h\check{z}\| &\leq \frac{\|h\|\|z\|}{V_M} \leq \|h\|(\delta\|u(t)\| + u_{\min}),\\ &= \delta\|u(t)\|\|h\| + u_{\min}h\,\mathrm{sign}(h). \end{aligned}\tag{18}$$

Rewriting (17) using (18) and (13) as

$$\begin{aligned}\dot{V} &\leq \delta\|u(t)\|\|h\| + h\left\{\tfrac{u(t)}{V_M} - \dot{L} - \dot{\lambda} + d + u_{\min}\mathrm{sign}(h)\right\} - \tfrac{1}{\varsigma}\tilde{b}\dot{\hat{b}},\\ &\leq \delta\|u(t)\|\|h\| + h\left\{\frac{u(t)}{V_M} + \mathcal{L}(\cdot)\right\} - \frac{1}{\varsigma}\tilde{b}\dot{\hat{b}}. \end{aligned}\tag{19}$$

Substituting the guidance control from (16) into (19) to obtain

$$\begin{aligned}\dot{V} &\leq \delta\left\|-kh - \left(\hat{b}\Theta + \mu(t)\right)\frac{h}{\|h\|+\phi}\right\|\|h\|\\ &\quad + h\left\{-kh - \left(\hat{b}\Theta + \mu(t)\right)\frac{h}{\|h\|+\phi} + \mathcal{L}(\cdot)\right\} - \frac{1}{\varsigma}\tilde{b}\dot{\hat{b}},\\ &\leq \delta k\|h\|^2 + \delta(\hat{b}\Theta + \mu(t))\|h\| - \left(\hat{b}\Theta + \mu(t)\right)\frac{\|h\|^2}{\|h\|+\phi}\\ &\quad - k\|h\|^2 + b\Theta\|h\| - \frac{1}{\varsigma}\tilde{b}\dot{\hat{b}}, \end{aligned}\tag{20}$$

where value of $\|\mathcal{L}(\cdot)\|$ from (15) and $h^2/(\|h\|+\phi) \leq \|h\|$ are used in the above equation. Further, note that

$$\frac{\|h\|^2}{\|h\|+\phi} = \|h\| - \frac{\phi\|h\|}{\|h\|+\phi} \geq \|h\| - \phi. \tag{21}$$

Substituting (21) and the value of $\dot{\hat{b}}$ into (20) gives

$$\begin{aligned}\dot{V} &\leq \delta k\|h\|^2 + \delta(\hat{b}\Theta + \mu(t))\|h\| - (\hat{b}\Theta + \mu(t))(\|h\| - \phi)\\ &\quad - k\|h\|^2 + b\Theta\|h\| - \frac{1}{\varsigma}\tilde{b}\mathbf{Pr}\left\{\frac{\varsigma\|h\|^2\Theta}{\|h\|+\phi}\right\},\\ &\leq -k(1-\delta)\|h\|^2 + \delta(\hat{b}\Theta + \mu(t))\|h\| + \tilde{b}\Theta\|h\| - \mu(t)\|h\|\\ &\quad + (\hat{b}\Theta + \mu(t))\phi - \frac{\tilde{b}\|h\|^2\Theta}{\|h\|+\phi}, \end{aligned}\tag{22}$$

where projection property, i.e., $-(1/\varsigma)\tilde{b}\mathbf{Pr}(\cdot) \leq -(1/\varsigma)\tilde{b}(\cdot)$ is used in the above inequality. Also, note that

$$\tilde{b}\Theta\|h\| - \frac{\tilde{b}\|h\|^2\Theta}{\|h\|+\phi} = \tilde{b}\Theta\phi\frac{\|h\|}{\|h\|+\phi} \leq \tilde{b}\Theta\phi. \tag{23}$$

Substituting (23) into (22) while using $\tilde{b} = b - \hat{b}$ yields

$$\begin{aligned}\dot{V} &\leq -k(1-\delta)\|h\|^2 + \delta(\hat{b}\Theta + \mu(t))\|h\| - \mu(t)\|h\| + (b\Theta + \mu(t))\phi,\\ &= -k(1-\delta)\|h\|^2 - \{\mu(t)(1-\delta) - \delta\hat{b}\Theta\}\|h\| + (b\Theta + \mu(t))\phi. \end{aligned}\tag{24}$$

Applying the value of $\mu(t)$ into (24) gives

$$\dot{V} \leq -k(1-\delta)\|h\|^2 + (b\Theta + \mu(t))\phi. \tag{25}$$

The upper bound value of $(b\Theta + \mu(t))\phi$ can be determined by substituting the value of $\mu(t)$ and ϕ in it as

$$\begin{aligned}&= \left[\tfrac{\delta\,\hat{b}\,\Theta}{1-\delta} + \varpi + b\Theta\right]\tfrac{\zeta}{1+\Theta} = \left[\tfrac{\delta\,\hat{b}\,\zeta}{1-\delta} + b\zeta\right]\tfrac{\Theta}{1+\Theta} + \tfrac{\zeta\varpi}{1+\Theta},\\ &\leq \frac{\delta\,\hat{b}\,\zeta}{1-\delta} + b\zeta + \zeta\varpi. \end{aligned}\tag{26}$$

Substituting (26) into (25) gives the following

$$\dot{V} \leq -k(1-\delta)\|h\|^2 + \frac{\delta\,\hat{b}\,\zeta}{1-\delta} + b\zeta + \zeta\varpi. \tag{27}$$

Since the estimate of b is bounded, therefore $\tilde{b} = b - \hat{b}$ is also bounded with a bound $|\tilde{b}| \leq \psi$, where ψ is a constant. Therefore, the Lyapunov function V can also be written as

$$V \leq \frac{1}{2}\|h\|^2 + \frac{1}{2\varsigma}\psi^2,\ \text{or,}\ \|h\|^2 \geq 2V - \frac{\psi^2}{\varsigma}. \tag{28}$$

Substituting the value of $\|h\|^2$ from (28) into (27) yields

$$\dot{V} \leq -2k(1-\delta)V + \frac{k(1-\delta)\psi^2}{\varsigma} + \frac{\delta\,\hat{b}\,\zeta}{1-\delta} + b\zeta + \zeta\varpi. \tag{29}$$

Defining $\eta = \frac{k(1-\delta)\psi^2}{\varsigma} + \frac{\delta\,\hat{b}\,\zeta}{1-\delta} + b\zeta + \zeta\varpi$. Since all the parameters of η in the right hand side are bounded, therefore η is also bounded.

The equation (29) can be written as:

$$\dot{V} \leq -2k(1-\delta)V + \eta. \tag{30}$$

The residue bound of V can be defined as

$$\lim_{t\to\infty}\ \sup\ V \leq \frac{\eta}{2k(1-\delta)}. \tag{31}$$

The ultimate bound of $h(t)$ can be determined from (31) as:

$$\|h\| \leq \sqrt{\frac{\eta}{k(1-\delta)}}. \tag{32}$$

As h converges to the small neighbourhood of zero, the missile will be on-course to hit the target without the need for any further corrective maneuver. The residual bound of the heading error can be further narrowed down by the use of an appropriate high gain k. □

5. SIMULATION RESULTS

The performance of the input quantized guidance scheme is verified by carrying out simulation studies on two different cases, namely the tail chase scenario and the head-on engagement. In the tail chase scenario, the target tries to evade the missile by moving away from the missile, whereas in the head-on engagement the target is heading towards the missile. These two cases both start with a high initial heading error of 170° for the missile. The targets are considered to be non-maneuvering in nature and thus their lateral accelerations are taken to be $a_T = 0$. The initial separation distance between the missile and the target is considered to be 20km, measured along the LOS. The

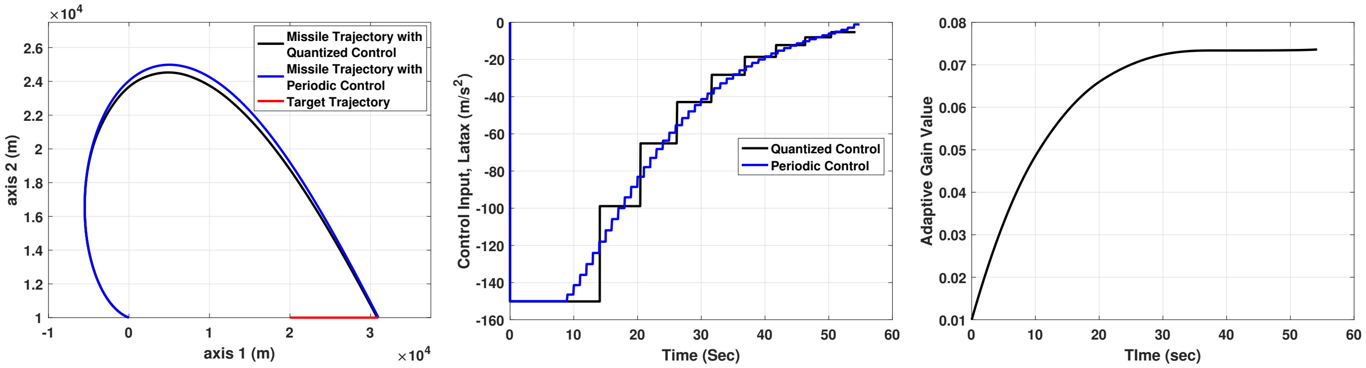

(a) Missile-target trajectories (b) The Latax profiles (c) The adaptive gain profile

Fig. 4. Simulation results for tail-chase scenario (Case 1)

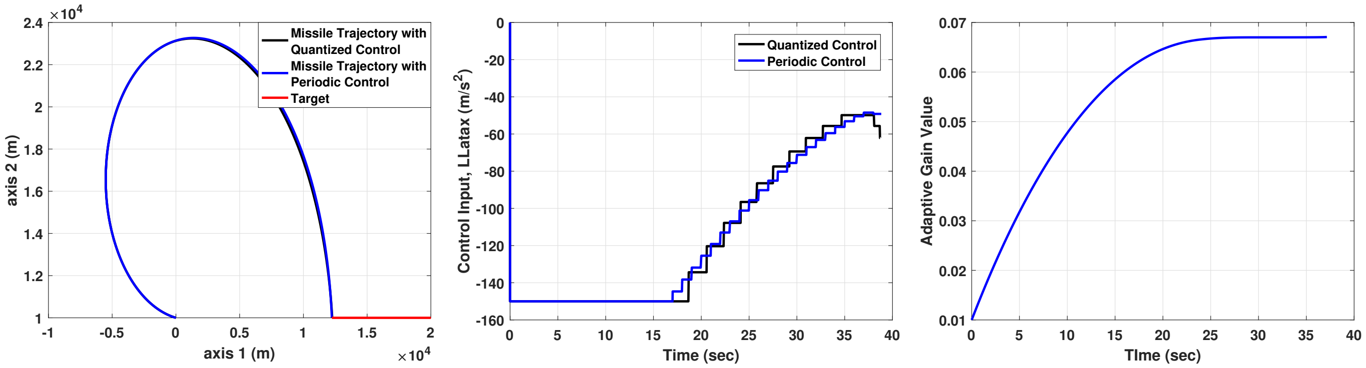

(a) Missile-target trajectories (b) The Latax profiles (c) The adaptive gain profile

Fig. 5. Simulation results for head-on engagement (Case 2)

initial lead angle and LOS angle are considered to be zero, i.e., $L(0) = \lambda(0) = 0°$. The tangential velocities of the target and missile are taken to be 200m/s and 1000m/s respectively. These model conditions are summarized in Table. 1. The external disturbance considered is time-varying in nature and consists of a constant part with two periodic components. It also consists of a high-frequency noise component which imitates the disturbance in sensory data. The uncertainty considered is expressed as

$$d = 0.05\left\{1 + \sin\left[\frac{\pi t}{250}\right] + \cos\left[\frac{\pi t}{250}\right] + 10^{-3}q\right\} \qquad (33)$$

Table 1.

Model Specifications for all Scenarios

Cases	V_M (m/s)	V_T (m/s)	a_T (m/s^2)	$\bar{u}$ (m/s^2)
Case 1	1000	200	0	150
Case 2	1000	200	0	150

Table 2.

Initial Conditions for Case 1 & 2

Cases	R_{T_1} (km)	R_{T_2} (km)	α_T (rad)	R_{M_1} (km)	R_{M_2} (km)	α_M (rad)
Case 1	20	10	0	0	10	$17\pi/18$
Case 2	20	10	π	0	10	$17\pi/18$

The initial position of the target and the missile along with their initial angle of attacks are summarized in Table. 2 for both the cases. The performance of the proposed guidance scheme using quantized control input and its comparison with periodically sampled technique as in (Wu, 2015) is presented in this section. The controller parameters for the quantized scheme are: $k = 0.0895$, $\delta =$, $u_{\min} = 1\mathrm{m/s^2}$, $\varpi = 0.0099$, $\varsigma = 0.0025$, $\zeta = 2.5$. The parameter γ is tuned to obtain better quantized control performance and has a value of $\gamma = 0.6586$. The rules for choosing these parameter values are in accordance with the rules presented in (Wu, 2015). For this scheme, the control input is updated periodically at a fixed sample time and not according to any predefined condition. Sampling time of $t = 1$ sec is considered for the periodic sample data technique, while the rest of the controller gains and parameter values are consistent with the ones used for the proposed input quantization guidance strategy.

5.1 Case 1

A tail chase scenario has been considered in this case and the performance comparison with the periodic sample approach is done based on three metrics, which include: 1) number of updates in the control input required for achieving the desired objective, 2) time of flight taken for interception of the target and 3) the fuel consumption. This comparison provides an insight into the efficiency of proposed quantized input approach in comparison to the widely used and traditional periodic sample approach. The periodic sample approach uses more than 6 times the updates required for the input quantization approach. The proposed approach is able to intercept the target faster and also consumes slightly lesser fuel as compared to the periodic sampled approach as can be seen in Table. 3. The missile-target trajectories for both the proposed quantized control approach and the periodic sample approaches are given in Fig. 4(a). The control input plots of these two guidance strategies are given in Fig. 4(b). The plot for the proposed adaptive gain during the time of flight is given in Fig. 4(c).

Table 3.

Performance Comparison for tail chase scenario

Method used	No. of updates	Fuel consumption	Time of flight
Proposed	9	100%	54.19
Periodic	55	100.25%	54.83

5.2 Case 2

The head-on engagement generally occurs more commonly in real-life scenarios than the tail chase scenario. Similar to the previous case nominal conditions are considered for the target. It is observed that the proposed approach outperforms the periodic sample approach in all performance matrices considered, i.e. it consumes slightly less fuel, has reduced time of flight and requires much less number of updates in control input. This performance comparison is summarized in Table. 4. The missile-target trajectories for the head-on engagement case are given in Fig. 5(a) and the latax plots are given in Fig. 5(b). The evolution of the adaptive gain value for the time of flight is given in Fig. 5(c).

Table 4.

Performance Comparison for head-on engagement

Method used	No. of updates	Fuel consumption	Time of flight
Proposed	13	100%	38.69
Periodic	39	100.44%	38.82

Remark 3. Even though in both the tail-chase and head-on engagement scenarios for the non-maneuvering cases discussed in this work, the periodic sampled approach consumes more fuel and takes more time to intercept the target as compared to the proposed approach, but this is not the primary motivation for this work. Further intuitively it can be assumed that if more cases were to be considered (i.e maneuvering target or otherwise), with varied initial conditions then the proposed control approach might not outperform the periodic sampled approach in these performance metrices. Nevertheless the proposed input quantization approach would still reduce the number of updates in control significantly, which is the primary motivation behind this work.

6. CONCLUSION

In this work, a logarithmic quantizer for guidance of a two-dimensional interceptor under constrained communication has been proposed. This guidance strategy reduces the updates of the control and is thus beneficial in reducing the communication load on the onboard processor of the missile. The proposed control law also tackles the external disturbances and quantization errors, encountered by the missile while capturing the target. The proposed logarithmic quantizer also ensures good precision for the quantized control system. Using Lyapunov theory, the UUB convergence of the closed-loop system states are proven. A comparative performance analysis between the proposed guidance strategy and the traditional periodic sampled data technique is performed. These results illustrate that the proposed guidance strategy outperforms the periodic sampled data technique on various performance metrics. For future work, the proposed approach can be applied to maneuvering and non-cooperative targets to verify its efficacy in those scenarios.

REFERENCES

Banerjee, A., Nabi, M., and Raghunathan, T. (2020). Time-energy optimal guidance strategy for realistic interceptor using pseudospectral method. *Transactions of the Institute of Measurement and Control*, 0142331220910919.

Bezick, S., Rusnak, I., and Gray, W.S. (1995). Guidance of a homing missile via nonlinear geometric control methods. *Journal of Guidance, Control, and Dynamics*, 18(3), 441–448.

Guo, J., Li, Y., and Zhou, J. (2019). A new continuous adaptive finite time guidance law against highly maneuvering targets. *Aerospace Science and Technology*, 85, 40–47.

Gurfil, P. (2003). Robust guidance for electro-optical missiles. *IEEE Transactions on Aerospace and Electronic Systems*, 39(2), 450–461.

He, S., Lin, D., and Wang, J. (2015). Continuous second-order sliding mode based impact angle guidance law. *Aerospace Science and Technology*, 41, 199–208.

Li, Y.X. and Yang, G.H. (2016). Adaptive asymptotic tracking control of uncertain nonlinear systems with input quantization and actuator faults. *Automatica*, 72, 177–185.

Moon, J., Kim, K., and Kim, Y. (2001). Design of missile guidance law via variable structure control. *Journal of Guidance, Control, and Dynamics*, 24(4), 659–664.

Pan, B., Fareed, U., Qing, W., and Tian, S. (2019). A novel fractional order pid navigation guidance law by finite time stability approach. *ISA transactions*.

Ramesh, S.H. and Padhi, R. (2019). Three-dimensional nonlinear gravity assisted aiming point guidance. *Aerospace Science and Technology*, 85, 505–513.

Shtessel, Y.B., Shkolnikov, I.A., and Levant, A. (2007). Smooth second-order sliding modes: Missile guidance application. *Automatica*, 43(8), 1470–1476.

Wu, B. (2015). Spacecraft attitude control with input quantization. *Journal of Guidance, Control, and Dynamics*, 39(1), 176–181.

Wu, B. and Cao, X. (2017). Robust attitude tracking control for spacecraft with quantized torques. *IEEE Transactions on Aerospace and Electronic Systems*, 54(2), 1020–1028.

Xing, L., Wen, C., Zhu, Y., Su, H., and Liu, Z. (2016). Output feedback control for uncertain nonlinear systems with input quantization. *Automatica*, 65, 191–202.

Yaghi, M.A. and Efe, M.O. (2019). H2/h∞ -neural based fopid controller applied for radar guided missile. *IEEE Transactions on Industrial Electronics*.